Journal of Structural Geology, Vol. 14, No. 10, pp. 1157 to 1172, 1992
Printed in Great Britain

0191-8141/92 $05.00+0.00
© 1992 Pergamon Press Ltd

Limitations of dimension and displacement data from single faults and the consequences for data analysis and interpretation

P. A. GILLESPIE, J. J. WALSH and J. WATTERSON

Department of Earth Sciences, University of Liverpool, P.O. Box 147, Liverpool L69 3BX, U.K.

(*Received* 22 *July* 1991; *accepted in revised form* 2 *April* 1992)

Abstract—The relationship between the maximum cumulative displacement on a fault (D) and the maximum linear dimension of the fault surface (W) is given by the expression $D = c\,W^n$, where the value of c is determined by rock properties; proposed values for n range from 1.0 to 2.0. Published datasets of D vs W measurements, together with new data, are presented in a common format. Most datasets are derived from maps and so the measurements of displacement and length do not represent maximum values for each fault. This factor, together with more than an order of magnitude range of c, causes regression on D vs W plots to be unsafe unless the range of W values plotted is *ca* 5 orders of magnitude. This restriction means that individual datasets must be combined to achieve the required range of fault size. Data analysis shows that the value of n must exceed 1.0 but discrimination between values of 1.5 and 2.0 cannot be made on the basis of data analysis alone. A modified fault growth model in which the increase in dimension of a fault with each slip event is proportional to $W^{0.5}$ gives rise to a value for n of 1.5. As this model has a sound mechanical basis 1.5 is the preferred value for n. The value of n influences other aspects of fault geometry, including the displacement profile on a fault surface, the spacing of depth contours on faulted horizons and the displacement populations of single fault surfaces.

INTRODUCTION

NUMEROUS datasets are available for investigation of the relationship between the dimensions of a fault surface and the maximum value of the fault offset, or displacement. Although the several investigators are agreed that the relationship is of the form

$$D = cW^n, \tag{1}$$

where D = maximum displacement, c = constant, related to material properties (including shear modulus) and W = fault dimension, proposed values of n range from 1.0 to 2.0 (Ranalli 1977, Watterson 1986, Villemin & Sunwoo 1987, Walsh & Watterson 1988, Scholz & Cowie 1990, Marrett & Allmendinger 1991, Cowie & Scholz 1992a,b). Evaluation of the data is complicated by lack of comparability of datasets, limited size ranges of faults within individual datasets, uncertainties regarding accuracy of data and by the lack of agreement on how the data should be analysed. Some authors have concluded that $n = 1.0$ while others have proposed values for n which exceed 1.0; other than agreement that a power-law relationship exists there is no concensus regarding further conclusions which can be drawn from the data. We have collated the relevant published data and present most of them, together with our own unpublished data, in a common format. The principal datasets considered are those given by the Minor Faults Research Group (MFRG, 1973), MacMillan (1975), Elliott (1976), Ranalli (1977), Ruzhich (1977), Muraoka & Kamata (1983), Krantz (1988), Walsh & Watterson (1988), Opheim & Gudmundssen (1989) and Marrett & Allmendinger (1991). We then consider the problems which arise in analysing the data and the consequent uncertainties which attend conclusions derived from the analysis. The main reason for wishing to obtain a reliable determination of n is that its value is a principal constraint on fault growth models which, in turn, are necessary for modelling strains within faulted volumes. The value of n also has a direct practical application in fault interpretation from seismic reflection data, in which minimum and maximum estimates of fault trace lengths can be used to choose between alternative fault correlations.

FAULT PARAMETERS

Dimensions

The linear dimensions of a single isolated fault surface are more easily defined than measured. In ideal cases the tip-line is a closed elliptical loop and the dimension used can be either a principal axis of the ellipse or the diameter of the equivalent circle. We define the maximum dimension of the fault plane in the direction perpendicular to the slip direction to be the width, W_m. The maximum dimension in the direction parallel to slip direction is defined as the length, L_m. In the case of normal faults and thrusts the width is horizontal and the length is in the vertical plane. These dimensions can be determined only in cases where the fault surface is mapped in three dimensions from either mine plan, seismic reflection or similar data, or by excavation of small faults in unconsolidated sediments. Most published data are derived from maps on which the fault trace lengths are measured (cf. length dimension of a fault surface). Fault traces on maps are chords on the fault surface, which are sub-parallel to the horizontal in the case of normal and reverse faults, with the chord lengths designated W_c, and are parallel to the length axis of strike-slip faults, with chord lengths designated L_c.

SG 14:10-D

Some outcrop data are available for chord lengths parallel to the down-dip, or length, axes of small normal faults. The maximum dimension of a fault is likely to be underestimated when derived from a map trace measurement. The mean value of chord dimensions on an elliptical fault surface is 0.75 of the principal axis to which the chords are parallel. W and L without subscripts refer to data for either maximum or chord dimensions or both where the distinction is either not possible or is unnecessary.

The concept of the single isolated fault is artificial insofar as it is strongly dependent on the scale of observation. The difficulty is partly resolved by the fact that a map of a given scale usually represents only faults with a limited range of sizes—usually spanning no more than 2 orders of magnitude of trace length. Even though fault traces represented by a single line on a map may be seen to consist of several individual elements when viewed on a larger scale map, the concept of a single fault is still useful when associated with a given scale. As fault systems appear to conform to the concept of geometrical coherence (Walsh & Watterson 1991) a small fault may be considered as a single fault at one scale but as a minor element of a larger fault when viewed on a different scale. Discontinuous, or segmented, traces of single faults with trace segments separated by relay zones (Larsen 1988) can be identified by the unusually high displacement gradients characteristic of segment tips (Walsh & Watterson 1990, Peacock 1991, Peacock & Sanderson 1991). Peacock (1991) has shown that for strike-slip faults developed within sandstone–shale sequences, fault segmentation is strongly influenced by lithology, with contractional relay zones in shales and extensional relay zones in sandstones (e.g. Peacock 1991, fig. 10); the displacement-dimension characteristics of individual fault segments is therefore sequence-related. Since the lengths and displacements of individual segments are not characteristic of the fault as a whole (Walsh & Watterson 1990, Peacock & Sanderson 1991), the array of segments is identified and treated as a single fault.

Regardless of scale, the length of a fault trace is defined as the distance between two tip-points at each of which the displacement is zero. Fault traces drawn on maps are usually underestimates of the total fault trace length as the regions of very low displacement close to the tips are frequently not recorded. Lengths of fault traces which are bounded by their intersections with other faults have no obvious significance, whether the other faults are of the same age with displacement transferred from one fault to the next, or whether the faults are of different ages. The inclusion of faults which intersect others in the same database may affect the apparent relation between D and W. For example, where fault branches occur, smaller displacement faults will usually be taken to be splays off larger displacement faults, and because they terminate at intersection (branch) points where displacement is not zero they should not be treated as independent faults: as branching splays have shorter trace lengths than isolated faults with the same D their inclusion in a dataset will lead to a lower estimate of the value for n (see below).

Displacements

An obvious displacement parameter is the maximum displacement (D_m) on the fault surface, which in the case of the ideal elliptical fault lies at the centre of the fault surface. This value can be accurately determined only where the fault surface has been mapped in three dimensions. In other cases the maximum displacement on a mapped fault trace (D_c) may be the only value obtainable. For a linear displacement profile from fault centre to tip, mean values of D_c on chords parallel to a principal axis of an elliptical fault surface will be $0.5D_m$, i.e. D_c underestimates D_m more than W_c underestimates W_m. D without subscripts refers to data for either D_m or D_c, or both where the distinction is either not possible or is unnecessary.

Another measure which could be used for displacement is the mean value of the displacement on a fault surface. This parameter has the advantage of being more easily compared with values of mean slip on a fault surface during a seismic slip event (u) which is the parameter usually used by earthquake seismologists. However, the difficulty of obtaining the mean value of displacement on a fault surface, or even along a fault trace, is even greater than that of determining the maximum displacement value.

As a general rule, displacements are most easily measured on dip-slip faults in sedimentary successions with low bed dips. Measurement of displacements on strike-slip faults is difficult in most rock sequences and estimates of maximum displacements on strike-slip fault traces are likely to be subject to relatively large errors. Good quality data are therefore likely to be biased towards dip-slip faults in sedimentary successions but such data are mostly limited to faults with maximum displacements of *ca* 5 km or less. Ambiguity occurs where a significant proportion of the fault displacement is accommodated by continuous deformation, or fault drag, rather than by slip on a fault surface discontinuity. In such cases the recorded displacement should include the continuous component. Similarly, where significant displacement is accommodated by continuous deformation the fault dimension should include the extent of any 'roll', or fold, occurring at the lateral tip of the trace of a fault discontinuity.

An additional complication is the inclusion of faults which intersect boundaries between strongly contrasting lithologies in which displacement is accommodated by different yield processes in the different lithologies. Such faults may be included in some of the published datasets. Faults may terminate abruptly at the boundary of a competent unit, at which there is still significant displacement, with a very incompetent unit which accommodates displacement by flow across the fault plane and a change of layer thickness. In such a case, displacement variation may be negligible along the fault surface within the competent layer. In circumstances

where the linear dimension of a small fault of this type is on a scale comparable with that of the lithological layering, the structure is best regarded as a type of boudinage rather than as a fault.

Data limitations

The relationship between displacement and dimension is believed to be dependent on the mechanical properties of the faulted rocks (Walsh & Watterson 1988). Ideally, D vs W data would be classified according to rock type and a dataset of this type would certainly be of great value. However, even small faults are rarely contained within a uniform rock type and only the broadest of rock classifications can be used to characterize each dataset: for most datasets the only useful distinction which can be made is between faults in sedimentary cover sequences and those in metamorphic basement rocks.

Given the inherent difficulties attached to measurement of the parameters of interest and to assessing the quality of an individual set, it might be thought that little purpose would be served by collecting and attempting to interpret these types of data. The single, but overriding, factor in favour of a more positive view is the wide range of fault sizes which occur. As with some other geological structures, fault sizes span a considerable range and recognizable faults have maximum displacements ranging over at least 8 orders of magnitude, i.e. from 1 mm to 100 km. In a dataset spanning only a small range of D and W, inaccuracies of measurement and the effects of multivariate control of the D vs W relationship may obscure the existence of a simple relationship between the two principal variables. The effects of additional variables and of inaccuracies of measurement are of much less significance when a wider size range of data is examined.

The use of data spanning several orders of magnitude of fault size introduces two further problems, however. The first of these problems is that no dataset assembled from a single source (e.g. a map) or acquired by a single method (e.g. by examination of outcrops, mine plans, seismic reflection profiles) is likely to span a sufficient range of fault size. Combining datasets from different sources inevitably degrades the data to some extent. The second problem is that data spanning several orders of magnitude of fault size can only be plotted using logarithmic scales, which can be deceptive. D vs W data distributions on log–log plots will inevitably show some areas of the plot to be devoid of data, because faults with the geometries appropriate to these areas would not be recognized and recorded even if they existed. The significance of some blank areas of the plots is therefore uncertain and their existence may lead to concentrations of data points being accorded greater significance than is merited. An ancient fault with large W/D ratio, e.g. W = 100 km and D = 10 m, is most unlikely to be recognized as such. If however the displacement is as large as 100 m for a 100 km fault width, then it is possible that the fault might be recognized because smaller faults with similar

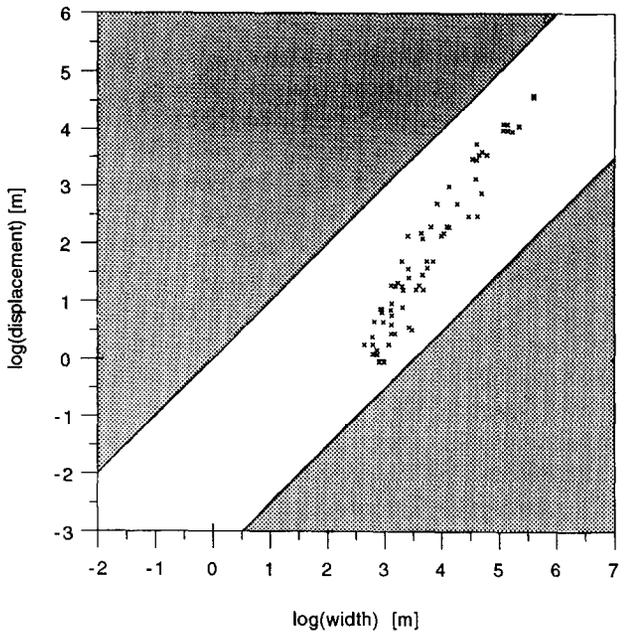

Fig. 1. Logarithmic plot of displacement (D_m) vs width (W_m) for faults (dataset 2), from Walsh & Watterson (1988). Also shown are those areas (stippled) which, following the assumptions outlined in the text, are inevitably devoid of data.

W/D ratios have been measured. The highest measured W/D ratio (*ca* 3000) derives from coal mine plan data and it is considered very unlikely that higher ratios would be measured from the other available data sources. The length of a fault in the slip direction (L_m) places an upper limit on the value of D for that fault, so that for a circular fault (W/L = 1) W/D must be greater than 1. Those areas of D vs W plots which are inevitably devoid of data are shown in Fig. 1 (assuming a circular fault), together with fault data from Walsh & Watterson (1988), where the bounding curves show why the concentration of data points must be interpreted with caution.

DISPLACEMENT–DIMENSION DATA

Datasets used

Data are from normal faults, strike-slip faults and thrusts, and are derived from a variety of sources. Datasets included in the statistical analysis are grouped as follows.

(1) A British coalfield dataset as described in Walsh & Watterson (1988). The dataset contains D_m vs W_m data for 34 fault radii and D_c vs W_c data for 518 fault traces (Fig. 2a). The estimated shear modulus for the rocks containing these faults is 3–10 GPa.

(2) A mixed dataset providing what are believed to be D_m vs W_m data for 70 normal faults and thrusts (Fig. 2b). This dataset contains some coalfield (contoured faults from dataset 1) and non-coalfield fault data listed in Watterson (1986), Barnett *et al.* (1987) and Walsh & Watterson (1989), including 20 thrusts in the Canadian Rockies from Elliott (1976). With the exceptions of the

British Coalfield and the Canadian Rockies datasets, both of which are considered later, datasets are too small for individual statistical analysis. The wide range of rocks from which this combined dataset derives have estimated shear moduli within the range 3–30 GPa.

(3) A mixed dataset (Fig. 2b) comprising 38 fault traces listed in table 1 of Walsh & Watterson (1988) and six normal fault traces from Krantz (1988). Two datasets listed in table 1 of Walsh & Watterson (1988) are not included: reactivated synsedimentary faults from Arizona–Utah (Babenroth & Strahler 1945) and small faults in semi-consolidated sediments from Japan (Muraoka & Kamata 1983). The synsedimentary faults are excluded because the displacements recorded at the contemporary surface or on older synfaulting horizons only represent minimum estimates of the cumulative displacement on the fault (synfaulting horizons have lower D/W ratios than prefaulting horizons and will follow a modified growth curve; Walsh & Watterson 1988). Since this dataset comprises fault traces contained within a variety of lithologies a representative estimate of shear modulus is not possible: shear moduli are however greater than 1 GPa.

(4) Values of D_c and L_c for 16 faults recorded by Muraoka & Kamata (1983) from Quaternary lacustrine deposits in Japan (Fig. 2c) for which the shear modulus has been estimated as 0.1–0.2 GPa (Walsh & Watterson 1988).

(5) A new dataset of D_c vs W_c for 53 normal faults in a North Sea oilfield (Fig. 2c), measured on subsurface horizon maps derived from three-dimensional seismic reflection data. The faults are imaged within a sequence of poorly lithified Mesozoic sandstones and siltstones for which the shear modulus of the entire sequence at the time of faulting is not known but is estimated as *ca* 3 GPa.

(6) Maximum offset (D_c) and fault trace length (L_c) data from 136 continental strike-slip faults (Fig. 2c) collated by MacMillan (1975) from the geological literature and analysed by Ranalli (1977, 1980). Estimates of length and, particularly, offset appear to be subject to large errors in some cases and no distinction is made between transcurrent and transform faults (Ranalli 1977). The effective shear modulus of rocks containing these faults is taken to be a value representative of the upper crust, i.e. 25–30 GPa. Direct comparison between this dataset and others can only be made if the relevant relationship between L and W is known: for combining with other datasets we assume, in the first instance, that $L = W$. The data plotted (Fig. 2c) are derived from tabulated datasets given by MacMillan (1975).

(7) Vertical displacement (D_c) and fault trace length (W_c) data for 78 normal faults measured from a 1:50,000 structure map of the Lorraine Coalfield by Villemin & Sunwoo (1987). The data plotted (Fig. 2d) were obtained by digitizing data points on the published diagram of Villemin & Sunwoo (1987). The effective shear modulus for rocks containing these faults is taken to be between 3 and 10 GPa, which is the appropriate range for British Coalfield strata of similar age. The dataset appears to include many fault traces terminated by intersection with other faults rather than by tip-points.

(8) Measurements of D_c and W_c for 22 normal faults in the Ruhr ($n = 12$) and South Wales ($n = 10$) coalfields (Fig. 2e) (Gillespie in press). The shear modulus for the rocks containing these faults is estimated to be 3–10 GPa.

(9) Measurements of D_c and W_c for 13 thrusts in the Ruhr ($n = 9$), South Wales ($n = 2$) and Appalachian ($n = 2$) coalfields (Fig. 2e) (Gillespie in press). The shear modulus for the coalfield rocks is estimated to be 3–10 GPa. Although measurements of D_c and L_c for thrusts from the Ruhr coalfield are presented elsewhere (Gillespie in press), these data are not easily compared with other D–W data because they show a broad range of aspect ratios (W/L *ca* 3–18).

(10) Displacement and length data, assumed to represent D_c and W_c, for 62 faults from Baykal and Transbaykal (Ruzhich 1977); the data shown in Fig. 2(f) were obtained by digitizing a published plot (Ruzhich 1977, fig. 1). In terms of fault size the data fall into two distinct groups: large faults with displacements greater than 100 m which were measured from fault maps, and small faults with displacements less than 10 m measured at outcrop. Of the small faults only one has displacement greater than 2 m and since a description of the lithologies involved is not available it is possible that these are boudinage type structures: a boudinage origin, with flow of adjacent lithologies is suggested by the very high D_c/W_c ratios of some faults (e.g. one fault has a maximum displacement of 2 m and a fault trace length of 10 m). Representative shear modulus values for the volume containing the larger normal faults are difficult to estimate, but since the faults probably extend through much of the upper crust a relatively high shear modulus is likely (>10 GPa).

Additional datasets which have not been included in the statistical analysis are represented in Fig. 3. Two of these datasets (11 and 12) have recently been described and analysed in some detail by Marrett & Allmendinger (1991) and are here represented as fields rather than by data points for individual faults.

(11) D_c and W_c data for 242 normal fault traces in the Gulf of Mexico (Marrett & Allmendinger 1991). Data were obtained by Marrett & Allmendinger (1991) from subsurface horizon maps derived from an interpretation of seismic reflection data.

(12) D_c and W_c data for 130 surface fault traces (Fig. 3) of normal faults in Japan (Minor Faults Research Group 1973).

(13) D_c and W_c data for eight fault scarps in Iceland (Fig. 3) (Opheim & Gudmundssen 1989). In common with the synsedimentary faults referred to above, fault displacements at the contemporary surface are perhaps best regarded as minimum estimates of the cumulative displacement on the fault (see dataset 3). This small dataset is not included in Table 1 but the results of regression analysis are referred to later.

A dataset given by Menard (1962) is excluded because it includes several transform faults.

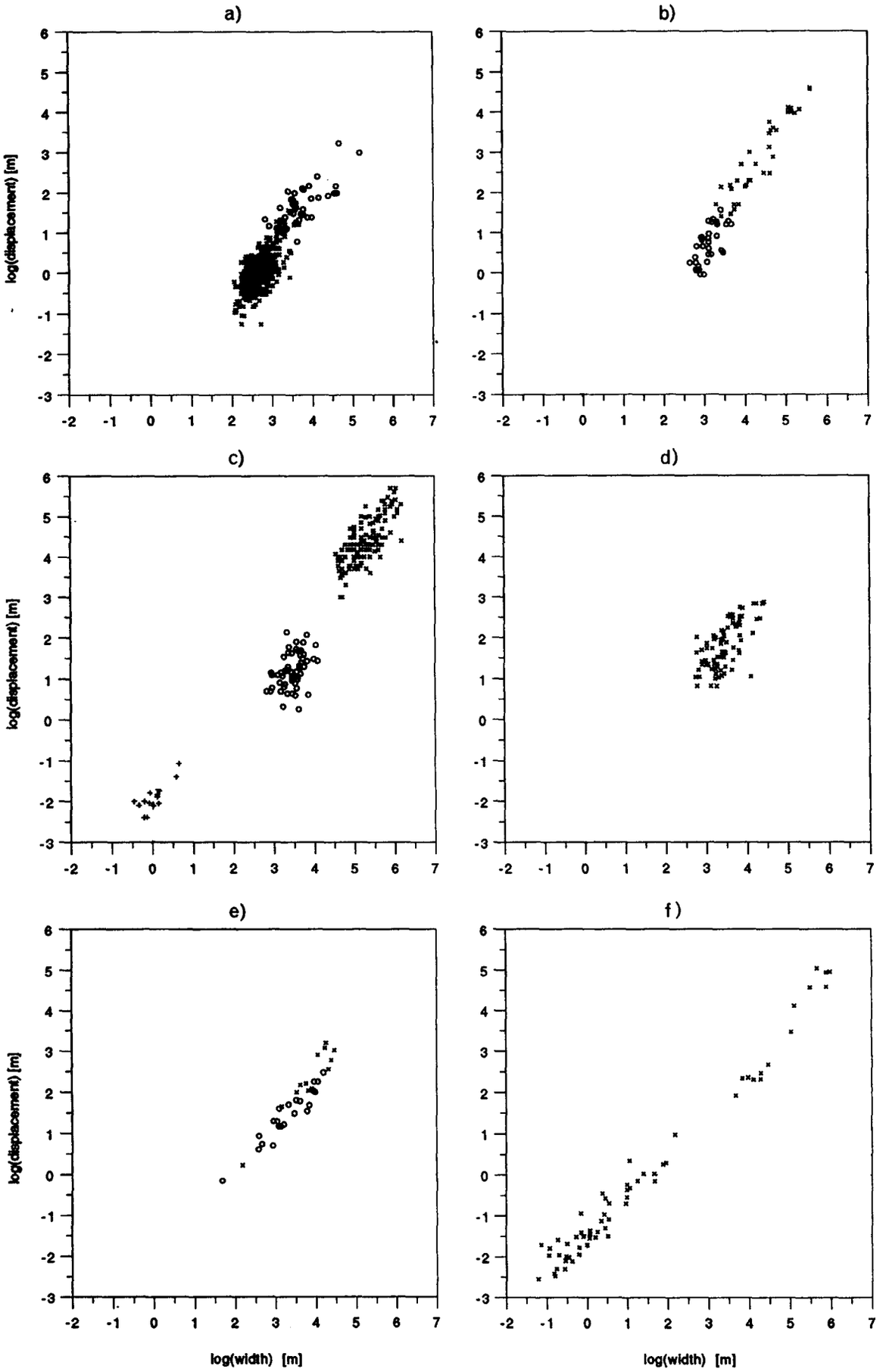

Fig. 2. Logarithmic plots of displacement vs width for various datasets: (a) D vs W_c, for datasets 1 (crosses) and 3 (open circles); (b) D_m vs W_m, for dataset 2 which includes contoured faults from dataset 1 (open circles); (c) D_c vs W_c for dataset 5 (open circles) and D_c vs L_c for datasets 4 (upright crosses) and 6 (diagonal crosses); (d) D_c vs W_c for dataset 7; (e) D_c vs W_c for datasets 8 (crosses) and 9 (open circles); (f) D_c vs W_c for dataset 10.

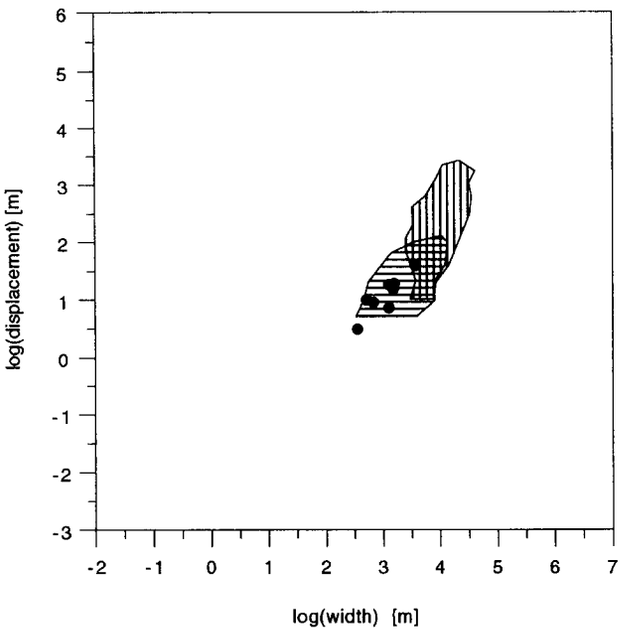

Fig. 3. Logarithmic plot of displacement (D_c) vs width (W_c) showing individual faults for dataset 13 (solid circles) and data fields for datasets 11 (vertical lines) and 12 (horizontal lines).

Statistical analysis of data

Table 1 shows statistical parameters for each individual analysed dataset and for various combinations of datasets. The results of regression analysis for D on W, W on D and for double regression (reduced major axis regression) are expressed as values of n, i.e. the exponent of W. Datasets with low correlation coefficients have narrow ranges of fault sizes and are characterized by large discrepancies between the values for n obtained by the three methods. All reduced major axis regression lines have $n > 1.0$ and, with three exceptions, $1.2 \leq n \leq 1.8$ for individual datasets. Individual datasets for which $n < 1.2$ are characterized by the following features: (i) dataset 3 is a mixed dataset and the regression line is dictated by one outlying data point, of 44, with high W and D; (ii) dataset 8 is small ($n = 22$) and the low value of n is representative of the data, although it is influenced by the inclusion of one small fault with W an order of magnitude smaller than W of the next largest fault; (iii) dataset 10, from the Baykal rift, comprises data which falls within two distinct fields (see above) with quite different regression lines. The low n value mainly derives from data for smaller faults (<2 m displacement), which could be boudinage structures, whereas larger faults provide a higher n value of 1.44, which is consistent with data from other areas.

Combined datasets also consistently provide values of n greater than 1.0, with values ranging from 1.4 to 1.85, except for those including datasets 4 and 10. Inclusion of dataset 10 (Baykal) leads to a decrease in n (although values remain >1.1) but since the nature of small faults within this dataset is not known inclusion of the data in combined datasets is considered inappropriate. The dataset from Quaternary lacustrine sediments (Muraoka & Kamata 1983) is excluded from all combined datasets because the shear modulus of the sequence containing the faults is over an order of magnitude less than that for all other datasets; material properties, including shear modulus, are an additional variable in the D vs W relation (i.e. c in equation 1). The consequences of producing combined datasets is illustrated for data from the British and Lorraine Coalfields (Fig. 4a) which, when combined give an order of magnitude

Table 1. Parameters characterizing individual and combined datasets (numbers denote datasets referred to in text). No.—number of data values in dataset. The range, minimum, maximum and mean values of log W (or where appropriate L, see text) and log D are provided for each dataset. The following statistical parameters are listed for each dataset: r_P—Pearson correlation coefficient; r_S—Spearman correlation coefficient; M_y—value of n for least-squares regression of log D on log W; M_x—value of n for least-squares regression of log W on log D; M_{xy}—value of n for reduced major axis, or double, regression

		log W				log D								
Dataset	No.	Range	Min	Max	Mean	Range	Min	Max	Mean	r_P	r_S	M_y	M_x	M_{xy}
1	552	1.62	2.05	3.67	2.65	2.78	−1.22	1.56	0.01	0.62	0.50	0.90	2.37	1.46
2	70	2.95	2.64	5.60	3.74	4.65	−0.05	4.60	1.80	0.96	0.94	1.59	1.72	1.65
3	44	2.36	2.83	5.18	3.68	2.45	0.79	3.24	1.66	0.74	0.67	0.75	1.39	1.02
4	15	1.12	−0.52	0.60	−0.02	1.35	−2.40	−1.05	−1.91	0.78	0.60	0.94	1.54	1.20
5	53	1.15	2.85	4.00	3.46	1.70	0.30	2.00	1.18	0.43	0.44	0.64	3.52	1.50
6	136	1.63	4.54	6.18	5.28	2.70	3.00	5.70	4.40	0.73	0.71	1.05	1.94	1.43
7	78	1.69	2.74	4.43	3.46	2.07	0.81	2.88	1.81	0.67	0.66	0.94	2.11	1.41
8	22	2.52	1.68	4.19	3.30	2.64	−0.15	2.48	1.44	0.95	0.93	0.97	1.08	1.02
9	13	2.27	2.18	4.46	3.81	2.90	0.30	3.20	2.31	0.95	0.84	1.19	1.32	1.25
10	62	7.20	−1.21	5.98	1.26	7.56	−2.52	5.04	−0.15	0.99	0.97	1.00	1.03	1.02
1—faults	34	1.02	2.64	3.67	3.10	1.61	−0.05	1.56	0.68	0.69	0.70	1.23	2.60	1.79
1—fault traces	518	1.51	2.05	3.56	2.62	2.46	−1.22	1.24	−0.03	0.52	0.43	0.74	2.75	1.43
1,2,3	632	3.54	2.05	5.60	2.82	5.82	−1.22	4.60	0.29	0.91	0.66	1.43	1.74	1.58
1,7	630	2.80	2.05	4.43	2.75	4.10	−1.22	2.88	0.23	0.82	0.65	1.50	2.25	1.84
6,7,10	276	7.39	−1.21	6.18	3.87	8.22	−2.52	5.70	2.65	0.98	0.95	1.11	1.16	1.14
1–3,5–10	996	7.52	−1.22	6.30	3.17	8.22	−2.52	5.70	1.04	0.93	0.89	1.32	1.53	1.42
1–3,5–9	934	4.62	1.68	6.30	3.29	6.92	−1.22	5.70	1.12	0.96	0.88	1.58	1.71	1.65
2,6,7,10	346	7.39	−1.21	6.18	3.84	8.22	−2.52	5.70	2.47	0.96	0.96	1.13	1.22	1.18
1,2,3,6,7	846	4.12	2.05	6.18	3.28	6.92	−1.22	5.70	1.09	0.97	0.85	1.60	1.71	1.65
2,6,7	284	3.53	2.64	6.18	4.40	5.74	−0.05	5.70	3.05	0.95	0.94	1.46	1.61	1.53

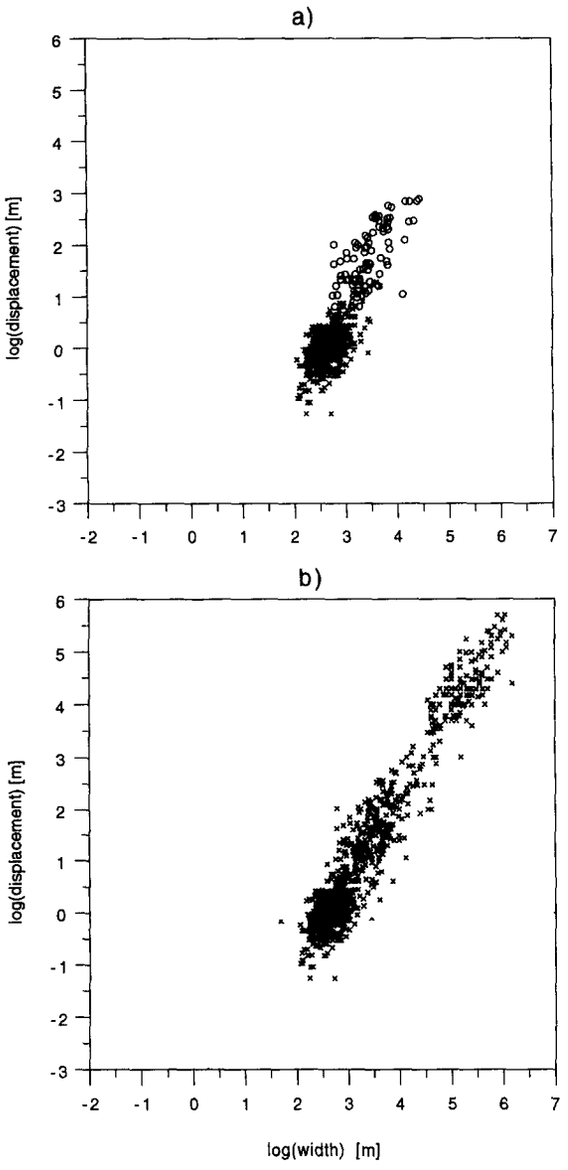

Fig. 4. Logarithmic plots of displacement (D_c) vs width (W_c) for combined datasets. (a) Combined coalfield dataset (datasets 1 and 7). (b) Main combined dataset (datasets 1–3 and 5–9; dataset 2 is for D_m vs W_m and dataset 6 is for D_c vs L_c).

increase in the ranges of D and W relative to those for the individual datasets, with consequent increase in the value of n to 1.84. Combining data for all faults in rocks with shear moduli greater than 1 GPa (Fig. 4b) gives a value for n of 1.637; Baykal data are not included in this combined dataset because rock types are unknown.

The robustness of the relationship between D and W can be tested in other ways. The potential shortcomings of individual datasets can be identified and then quantified in terms of their likely effects on any derived value of n. The effect of omission of certain datasets from combined datasets can also be quantified. These testing procedures have been performed in the following ways on a combined dataset which includes all but two (4 and 10) of the individual datasets.

(i) The dimensions of strike-slip faults in dataset 6 are chords measured parallel to the slip direction (i.e. L_c). For direct comparison with other datasets, for which the chords are perpendicular to the slip direction (W_c), an estimate is required of the L:W ratio of strike-slip faults. We have assumed in the first instance that $W = L$ (as in Fig. 2c and Table 1). The down-dip extent of large faults is however limited by the thickness of the seismogenic layer (i.e. for strike-slip faults W is fixed; Scholz 1982, 1990, Strehlau 1986) below which displacements are likely to be accommodated on a ductile shear zone. At greater depths displacement decrease on a ductile shear zone can be accommodated either by pure shear or by transfer to other shear zones and the combined dimension of the fault and shear zone is therefore not appropriate for comparison of L and W data. The parameter required is that which describes the equivalent relation between L and W on individual faults bounded by tip lines i.e. the relation between the slip-parallel (edge dislocation) dimensions and the slip-perpendicular (screw dislocation) dimensions of faults. For this we use the L:W ratio established for faults for which we have displacement measurements over the entire surface (*ca* 1:2; Walsh & Watterson 1989). The effect of assuming a W/L ratio similar to that for other faults (i.e. 2.0), is a decrease in the value of n from 1.65 to 1.52 (Fig. 4).

(ii) Chord data from British coalfields represent one of the better quality datasets because they are derived from mine plans (dataset 1; Walsh & Watterson 1988). The large number of data points within this dataset has a significant influence on the best fit regression line such that exclusion of the dataset leads to a decrease in n from 1.65 to 1.563 (Fig. 4a).

(iii) Applying the restrictions in both (i) and (ii) results in a decrease in n from 1.65 to 1.40.

(iv) Although inclusion of the Baykal dataset is considered inappropriate, for the reasons previously outlined, a combined dataset including these data, together with the restrictions in both (i) and (ii), still gives a value of n which is significantly greater than 1.0 (i.e. $n = 1.15$; Fig. 5). If this dataset is omitted, as we believe it should be, the values of n obtained by regression for all combined datasets are >1.4.

Figure 6 shows the field containing most of the data points for all datasets excluding 4 and 10. Also shown are fields for data from Marrett & Allmendinger (1991), which are consistent with all other datasets, in respect of both position and trend (Fig. 6).

Limitations of statistical analysis

The purpose of this section is to consider the usefulness of regression analysis in establishing the value of n, as opposed to developing a predictive tool. The standard method of determining the value n for an individual dataset is to calculate the best-fit line through the data points. Although we give values for n derived in this way, we have previously expressed doubts about application of this procedure to data of this type (Walsh & Watterson 1988) and these doubts remain. There are two distinctive features of the data which must be taken into account, neither of which is uncommon in geological datasets.

The first feature is that although the standard pro-

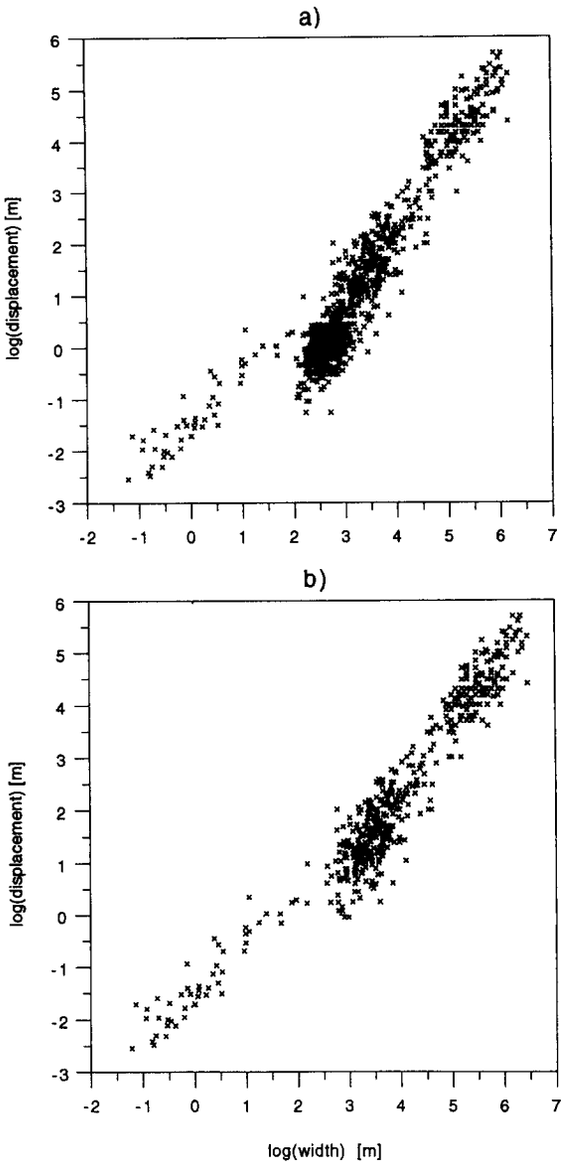

Fig. 5. Logarithmic plots of displacement (D_c) vs width (W_c) for combined datasets. (a) Combined dataset (datasets 1–3 and 5–10; dataset 2 is for D_m vs W_m and dataset 6 is for D_c vs L_c). (b) As in (a) but with dataset 1 omitted and with dataset 6 replotted assuming $W = 2L$ (see text for details).

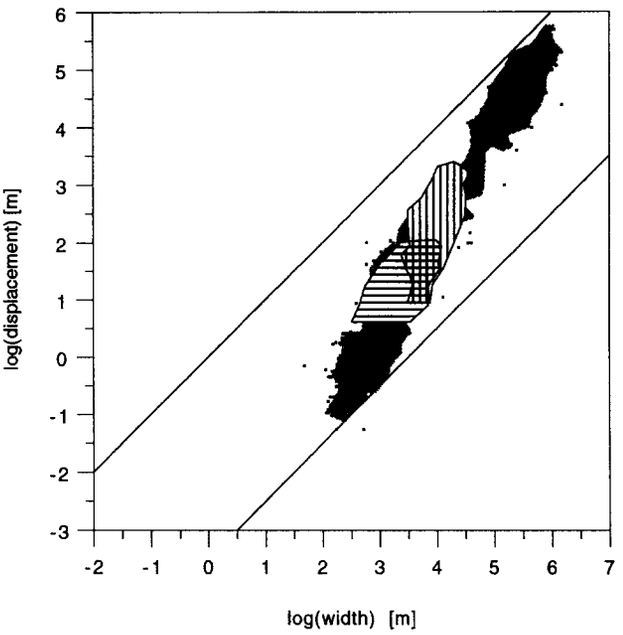

Fig. 6. Logarithmic plot of displacement vs width showing the main field (shaded) for the combined dataset (datasets 1–3 and 5–9) together with the superimposed fields for datasets 11 (vertical lines) and 12 (horizontal lines). Also shown are individual data points for those faults in the combined dataset which plot outwith the main field, and a pair of parallel lines which bound the field within which measurable W/D ratios occur.

cedure for regression analysis is to regress y on x where x is the independent variable, it is not obvious in this case whether D or W is the independent variable. In such circumstances, regressing y on x is arbitrary and reduced major axis regression is necessary. Reduced major axis regression (Davis 1986), hereafter double regression, minimizes the product of the deviations in x and y, and is a commonly used technique in the study of growth of organisms (biometry) where it is also not possible to decide which variable should be x and which variable should be y. From Table 1 it can be seen that for the several individual and combined datasets there are significant differences between the slopes of best-fit lines determined by regressions of D on W, W on D and by double regression. These differences are an indication of the importance of the second feature of the datasets which must be taken into account, as follows.

An implicit assumption of regression analysis is that the data represent a system with only one degree of freedom, i.e. for any value of x there is ideally only a single corresponding value of y. D vs W data are not of this type because the relationship between D and W is influenced by other variables (e.g. shear modulus), the effects of which are shown by variation in the value of the constant, c. Walsh & Watterson (1988) claimed that the shear modulus of the rocks containing a fault exercises a significant, although limited, control on the D vs W relation. Regardless of whether or not shear modulus has the significance claimed for it, the potential influence of one or more additional variables must be considered. If the effects of one or more additional variables are present in the data then D vs W data points will not be expected to lie along a line but to lie within a band; the width of the band will depend on the role and on the range of the additional variable(s). The potential band width of D vs W data distributions is also increased by a number of factors which include: (i) the use of chord data (fig. 4, Walsh & Watterson 1988); (ii) the effect of errors in measurement; and (iii) the inclusion of segmented faults and branching splays. We know of no statistical method which permits definition of the best-fit band.

Most of the datasets show a band distribution with the width of the band approximately equivalent to an order of magnitude variation in W. Regardless of the reason for this distribution, it is evident that a meaningful estimate of n cannot be derived from any dataset which does not span several orders of magnitude of D and W. Datasets which span only 1 or 2 orders of magnitude variation in D and W, which is the case with most of the

individual datasets, will inevitably give misleadingly low values of n when best-fit lines are calculated. We have investigated the effects of limited ranges of D and W on best-fit lines by constructing synthetic datasets. The datasets are formed by randomly distributing data points within rectangular bands of different aspect ratio but with 1 order of magnitude range of W for a given D. The data fields have aspect ratios ranging from 1 to 10 and slopes of 1.5 and 2.0 for the long axes of the rectangles; the number of data points increases linearly from 100 to 1000 with increasing aspect ratio. For an aspect ratio of 10 the data points span *ca* 5.5 orders of magnitude of W and *ca* 9.5 orders of magnitude of D, for a slope of 2.0, and 6.5 and 9.5 orders of magnitude of D and W, respectively, for a slope of 1.5. Slopes of best-fit lines for regressions of D on W, W on D and for double regression have been calculated for aspect ratios ranging from 1 to 10. The exercise was repeated several times for different random sets of data points and the results are relatively stable.

Typical results for slopes of 1.5 and 2.0 are shown in Fig. 7 and clearly demonstrate that best-fit lines, even those obtained by double regression, can be very misleading when applied to datasets of this type. Slopes derived by double regression analyses of datasets with aspect ratios ≤ 2.0 are in error by *ca* 0.5 or more and only at aspect ratios of ≥ 4.0 can accurate estimates of slope be made. No reasonably well constrained individual D vs W dataset has an aspect ratio greater than *ca* 4.0. While regression analysis cannot therefore provide an accurate value for n it clearly shows that $n > 1.0$ for the datasets in Table 1. Dataset 10 (Ruzhich 1977) has an aspect ratio of 10.7 but, for the reasons previously outlined, this dataset is thought not to be well constrained. Quantitative analysis therefore usually requires the use of a combined dataset, as in Watterson (1986) and Walsh & Watterson (1988). The use of combined datasets introduces a further problem, however, because the individual datasets are derived from different rocks. In general, the larger the faults in a dataset the higher the shear modulus of the rocks is likely to be. Fault data from outcrop are most likely to be for small faults in sedimentary sequences which may be poorly lithified, small to intermediate ($D <$ *ca* 100 m) sized faults within either lithified or moderately lithified sedimentary rocks are well represented in coalfield and oilfield data, whereas data for larger faults ($D \gg 100$ m) are generally derived from oilfield maps or surface

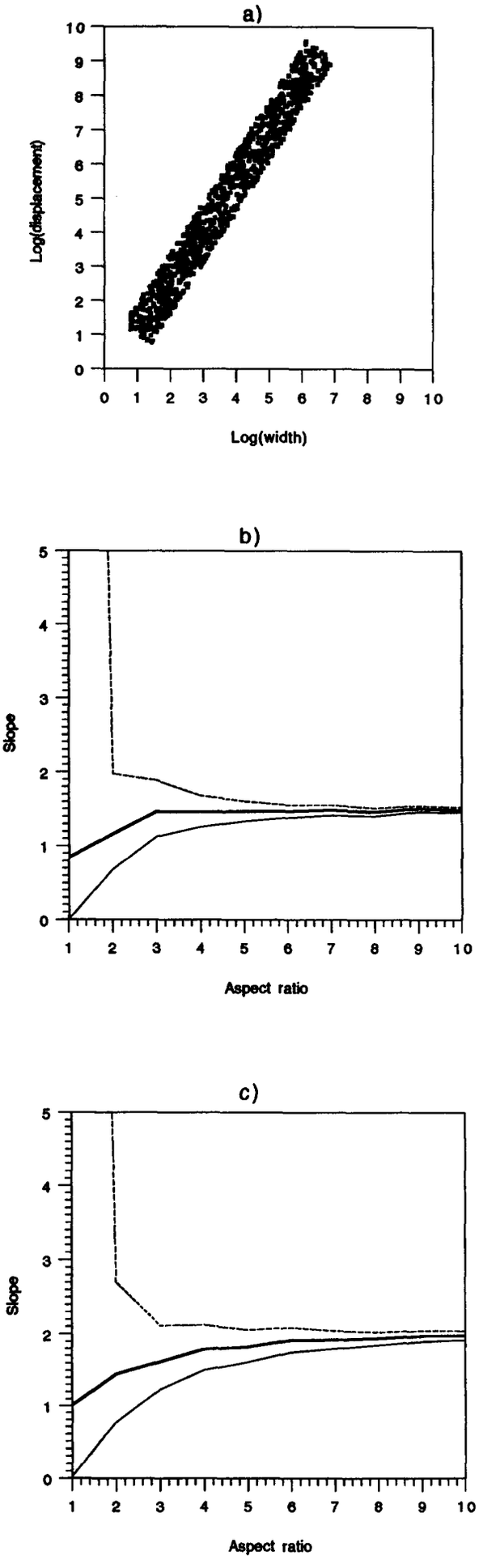

Fig. 7. (a) Synthetic dataset with band width of 1 order of magnitude of fault width and with aspect ratio of 10:1 and slope of 1.5 (see text for details). (b) Values of n derived from regression analysis performed on synthetic datasets, with band slope of 1.5, as shown in (a) but with a range of aspect ratios (1–10). Three curves are shown and represent different types of regression: regression of D on W (fine solid curve), W on D (broken curve) and double regression (heavy solid curve). (c) Values of n derived from regression analysis performed on synthetic datasets, with band slope of 2.0 and band width of 1 order of magnitude, but with a range of aspect ratios (1–10). Three curves are shown and represent different types of regression: regression of D on W (fine solid curve), W on D (broken curve) and double regression (heavy solid curve).

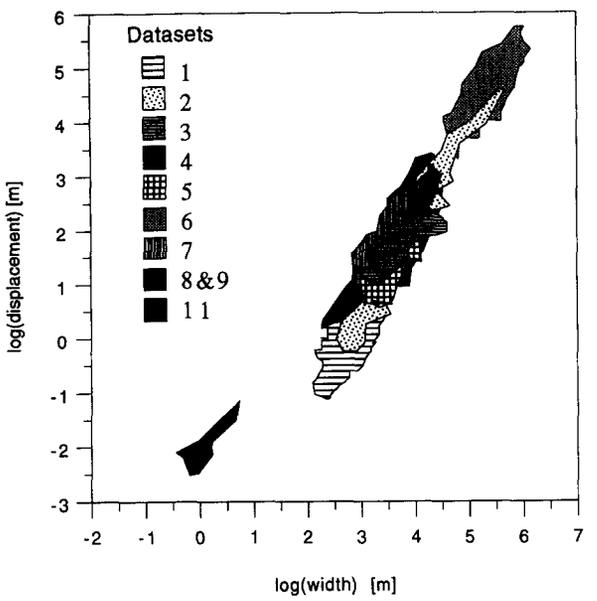

Fig. 8. Logarithmic plot of displacement (D) vs width (W) showing fields for individual datasets. Data fields for main datasets are shown: legend provides dataset numbers.

geological maps and are for faults which are likely to extend into or are entirely within metamorphic or other basement rocks. As has previously been pointed out (Walsh & Watterson 1988), a systematic variation of shear modulus with fault size is therefore to be expected and will introduce a systematic bias towards lower slopes of best-fit lines for the combined datasets. A related effect is that for small faults ($D < 10$ m) a wider range of shear moduli can be sampled because individual faults may be contained within single lithological units; for progressively smaller faults the band width of the available data will broaden. This effect is illustrated by the faults in dataset 4, which each occur within poorly lithified units dominated either by sand or by silt (Fig. 8).

Our belief is that, while the data clearly demonstrate that $n \gg 1.0$, a definitive choice between $n = 1.5$ and $n = 2.0$ cannot be made on the basis of statistical analysis of the data currently available. Given the quality and other characteristics of the data we believe that statistical analysis is of limited value and that the data can be examined most objectively by evaluating individual datasets as fields, as in Fig. 8. This procedure is not tantamount to ignoring the data, as has been suggested by Scholz & Cowie (1990), but is a necessary acknowledgement of the limitations of the data.

Previous estimates of n

The first suggestion of a systematic relationship between D and W was that of Menard (1962) which was based on data for strike-slip faults. Many of the faults for which data were presented are transform faults but nevertheless it was recognized that significant differences exist between small and large faults. Menard (1962) suggested that W/D ratios for small faults were approximately 7 and those for large faults approximately 3. In this context small faults were in the range 10–100 km and large faults up to 1500 km trace length. These values correspond to a value for n of *ca* 1.5. Elliott (1976), on the basis of data for Mesozoic thrusts in the Canadian Rockies proposed a constant W/D ratio of 14, i.e. $n = 1.0$; we have accessed these data by digitizing data points on published graphs and for double regression $n = 1.54$. Ranalli (1977), using the database compiled by MacMillan (1975), proposed that $n = 1.17$ on the basis of regression of D on W (for double regression $n = 1.43$, Table 1); the aspect ratio of the data field is *ca* 2.5. Ruzhich (1977) interpreted dataset 10 as indicating that $n = 1.18$ on the basis of regression analysis but, as shown above, faults with displacements greater than 2 m provide a value for n of 1.44. Villemin & Sunwoo (1987), using data from Lorraine coalfield maps, proposed that $n = 1.18$, apparently on the basis of regression of D on W (for double regression $n = 1.41$, Table 1); the aspect ratio of the data is *ca* 1.6. Watterson (1986) and Walsh & Watterson (1988) proposed that $n = 2.0$, as being within the range allowed by the data and as being the value which led to the simplest growth model. Opheim & Gudmundsson (1989) using data for small (<*ca* 50 m displacement) Icelandic fault scarps (dataset 13) suggest that $n = 1.0$ with a mean W/D ratio of 86; this dataset includes only eight faults but has a high aspect ratio (*ca* 4) and double regression provides $n = 1.06$. Scholz & Cowie (1990) proposed that $n = 1.0$ on the basis of individual consideration of six published datasets which, with the exception of one small dataset (dataset 13), have aspect ratios of < *ca* 3 (datasets 4, 6, 7 and 13, and the British coalfield and Canadian Rockies data included in dataset 2; Table 1). Marrett & Allmendinger (1991) used a combined dataset, which included datasets 6, 11 and 12 and data from Menard (1962), with an aspect ratio of *ca* 7.0 and suggested that $n = 1.5$, on the basis of regression of D on W giving a best-fit line of slope 1.46. This review shows that most authors have concluded that $n > 1.0$, albeit on the basis of datasets which generally have low aspect ratios. The original estimates are substantiated by double regression which provides estimates for n of >1.4 for all but one of the datasets (dataset 13).

VALUES OF *n* IN RELATION TO FAULT GROWTH MODELS

Significance of n

A systematic relationship between D and W for faults of different size would be unlikely unless a similar relationship existed between successive stages in the growth of individual faults. The value of n is thus a severe constraint on possible growth models. Alternatively, growth models can be used to discriminate between possible values for n within the range allowed by the data. This procedure has previously been used in proposing that $n = 2.0$, on the grounds that this value was both within the limits allowed by the data and also is the value consistent with the simplest growth model.

The crucial difference between various proposed values of n is that between proposals that $n = 1.0$ and proposals that $n > 1.0$ (see below); the primary objective of analysis of D vs W data must be to establish which of these alternatives is correct. In this section we describe a variety of growth models, preceded by a consideration of the earthquake seismological data which provide some constraint on single slip events on faults.

Earthquake data

Earthquake seismological studies have shown that there is a linear relationship between W and u for single slip events, such that the slip/width ratio for large intraplate faults is *ca* 6×10^{-5} (Scholz 1982, Scholz *et al.* 1986). For a given shear modulus, the slip/width ratio for a single slip event determines the stress drop (Δs). Stress drops are relatively constant over a broad range of earthquake size (*ca* 10 orders of magnitude, in terms of seismic moment M_o), with values generally ranging from 1 to 100 bars (Scholz 1990).

The stress drop for a circular fault is given by the expression

$$\Delta s = (7\pi G/16)u/R, \quad (2)$$

where G is shear modulus, u is slip and R is fault radius (Kanamori & Anderson 1975). Therefore the locus of single slip events for given shear moduli can be drawn for a given stress drop value. Earthquake curves are shown in Figs. 9(a) & (b) for stress drop values of 30 and 100 bars, for a range of shear moduli. Figure 9(c) shows the single field containing the main combined dataset (excluding dataset 10) and the field for dataset 4, and earthquake curves for $\Delta s = 30$ bars. The field of the main dataset shows only limited overlap with earthquake curves of appropriate shear moduli, i.e. 3–30 GPa. On the other hand, the field for dataset 4 straddles the earthquake curves for shear moduli equivalent to those of rocks containing the faults (0.1–0.2 GPa), an observation which suggests that the faults may be either single-slip events or may have grown in a limited number of events.

A variety of growth models is described below and the basic assumption in each of them is that the mean slip on a fault during a single seismic cycle (u) is directly proportional to the dimension of the surface over which the slip occurs, such that from (2)

$$u = kW, \quad (3)$$

where k is a constant through fault growth (i.e. for a given fault, stress drop (Δs) and shear modulus (G) are taken as constants). A requirement of this model is that when slip occurs on a fault it extends over the entire fault surface, a feature which is consistent with the maximum moment model (Wesnousky *et al.* 1983) and the characteristic earthquake model (Schwartz & Coppersmith 1984). These models postulate that individual faults and fault segments tend to generate earthquakes of essentially same size, i.e. characteristic earthquakes, that are a function of the fault length and tectonic setting. Be-

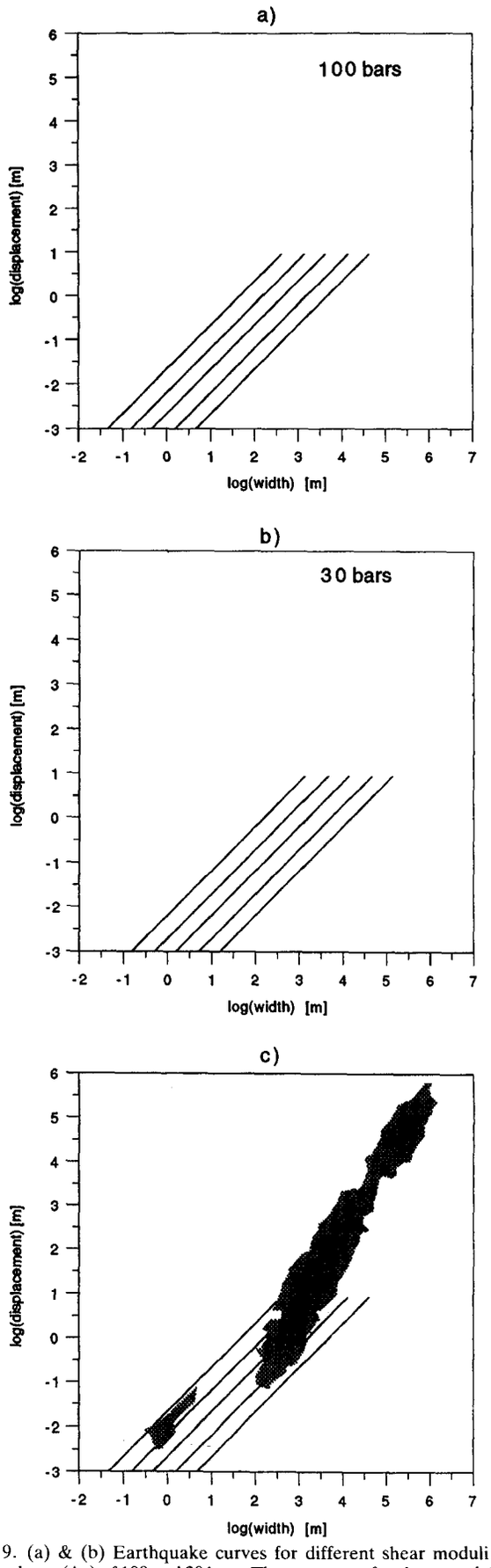

Fig. 9. (a) & (b) Earthquake curves for different shear moduli for stress drops (Δs) of 100 and 30 bars. The curves are for shear moduli of 30, 10, 3, 1 and 0.3 GPa: curves for higher shear moduli have lower D/W ratios. (c) Main field for combined dataset (datasets 1, 2, 3, 5, 6, 7, 8 and 9—stipple) and for dataset 4 (defining separate field with low D and W) together with earthquake curves for Δs of 30 bars for different shear moduli (10, 3, 1, 0.3 and 0.1 GPa).

cause log–log relationships are plotted, the plot is not sensitive to some departure from the assumptions of these models.

Growth models

The fault growth models described below differ from a direct application of linear elastic fracture mechanics in that the elastic strains which accommodate the dislocation on a fault resulting from a single slip event are relaxed into permanent strains before the next slip event (Watterson 1986, Walsh & Watterson 1988). Linear elastic fracture mechanics predicts that if these elastic strains are not relaxed $D \propto W^{0.5}$ (Scholz 1990), a relation which is inconsistent with available data (Walsh & Watterson 1988). The notion of stress (or elastic strain) relaxation is supported by the observation that the strains associated with large displacement faults are too high to be accommodated elastically (Watterson 1986). The basic assumption of our growth models is that the stress distribution following each slip event is the same in all but scale. Relaxation of these stresses, or elastic strains, by permanent straining due to, for example, small-scale fracturing and pressure solution, can also be effected at the tip-line of the fault, where the highest elastic strains are imposed, either by fracture propagation accompanying the slip event or by subcritical fracture propagation between slip events (Walsh & Watterson 1988). The significant material property determining fracture propagation for a given initial stress distribution is fracture toughness, which varies over only *ca* 1 order of magnitude (Walsh & Watterson 1988). The growth models outlined below differ only in respect of the relation between the amounts of slip and fracture propagation during a single seismic cycle.

The value of n in the D vs W relation describes the change in fault geometry with growth. In common with allometric growth laws in biology an exponent of 1.0 indicates no shape change, with self-similarity of form, whereas other values describe a systematic change in shape with growth (Thompson 1917). If $n = 1.0$ faults not only have a much higher degree of geometrical similarity than if $n > 1.0$ but the increment by which u increases in successive slip events is linearly related to both D and W. If $n > 1.0$ then increments of increase in u are not linearly related to either D or W. If the fault dimensions remain constant while accumulating many slip events then $n = \infty$, which clearly is not the case. Any value of n which is less than infinity requires that W increases during the active life of a fault, i.e. a fault growth model is applicable. If n is constant during the growth of a fault, i.e. the D vs W values at successive stages in the growth of a single fault plot as a straight line on a log–log plot, then the fault growth sequence is severely constrained, as follows. The successive values of u during growth of a fault form a series and the sum of this series is the cumulative displacement, D, at each stage of growth.

In the arithmetic growth model (Watterson 1986, Walsh & Watterson 1988) amounts of slip in successive slip events have a common difference, the slip increment (a), such that for a large number of slip events

$$u_N = aN, \tag{4}$$

where u_N is the amount of slip in a slip event and N is the (large) number of preceding slip events. The relationship between the amount of slip in a single event and the dimension of the slip surface is given by

$$u_N = kW_N, \tag{5}$$

where W_N is the maximum dimension of the slip surface and k is a constant which probably varies with rock properties (Scholz 1982). A fault grown in accordance with the above two relationships satisfies the expression

$$D = cW^2, \tag{6}$$

where D is the maximum cumulative displacement, W is the final fault width and c is a constant which is dependent on material properties of which the most significant is shear modulus (Fig. 10). The simplest type of series whose sum is given by a power law of constant power, n, independent of the number of terms in the series is an arithmetic series where $n = 2.0$. Although this scaling law is quite simple, with a linear relationship between D and the fault surface area (W^2), there is no obvious mechanical reason why faults should grow in this way (Walsh & Watterson 1988).

However, the data do not demonstrate unequivocally that n is constant at all stages of fault growth and other series are compatible with the data. Some of these possibilities are illustrated in Figs. 11 and 12. Possible growth series are of two types, those which relate successive values of u, as in the growth models previously put forward (Watterson 1986, Walsh & Watterson 1988, Marrett & Allmendinger 1991, Cowie & Scholz 1992a,b), and those based on the difference, or increment, between successive values of u.

Growth models in which the successive slip events constitute a geometric series, i.e. $u_N = (u_{N-1})^i$, do not give rise to a power-law relationship between D and W and therefore are inconsistent with the data and for that reason were rejected.

What have not previously been investigated are growth models in which either the slip in successive events or the differences between slip in successive events constitute a p series, such that
in the first case

$$u_N = bN^i \tag{7}$$

and in the second case

$$u_N - u_{N-1} = b(u_{N-1})^i \tag{8}$$

or

$$u_N = u_{N-1} + b(u_{N-1})^i, \tag{9}$$

where b is a constant.

Numerical evaluation of the D vs W relationships for such series shows that, where N is large, they give rise to power-law growth curves with $D = cW^n$, where $n = (1 + 1/i)$ in the first case (Fig. 11) and $n = 2 - i$ in the

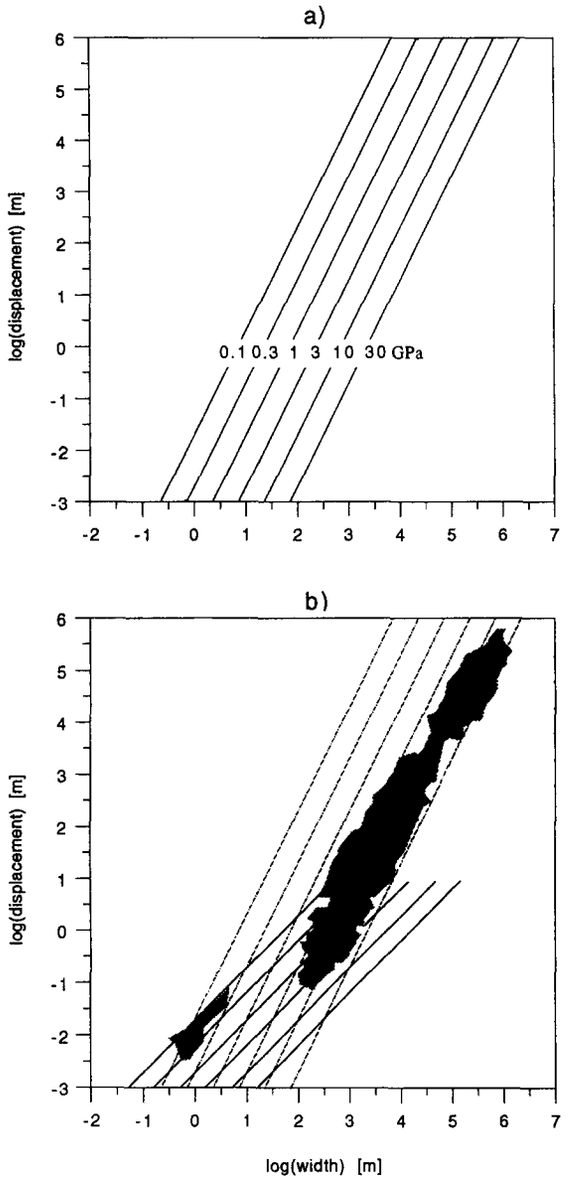

Fig. 10. Growth curves for arithmetic growth model (Walsh & Watterson 1988). Curves for faults contained within rocks of different shear moduli are shown (values are in GPa). (b) Main field for combined dataset, as in Fig. 9(c), growth curves for arithmetic growth model, as in (a), and earthquake curves for different shear moduli (as in a) for a stress drop (Δs) of 30 bars (see Figs. 9b & c).

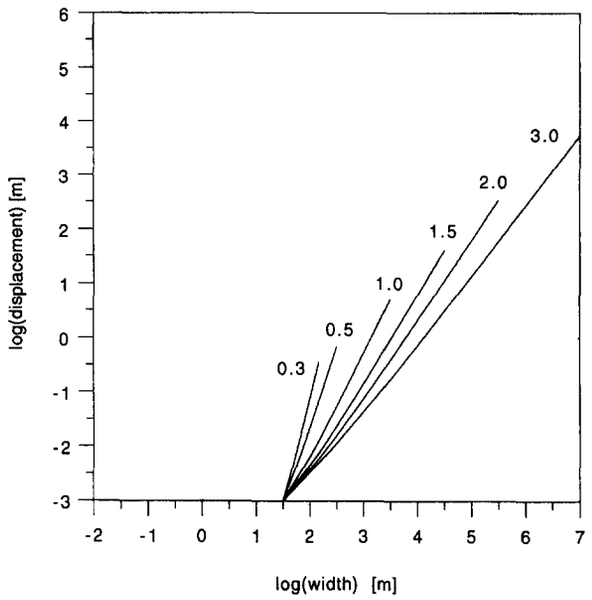

Fig. 11. Growth curves for model in which successive slip events form a p-series, such that $u_N = bN^i$, for i = 0.33, 0.5, 1.0, 1.5, 2.0 and 3.0. These models provide steady-state growth curves with $n = (1 + 1/i)$.

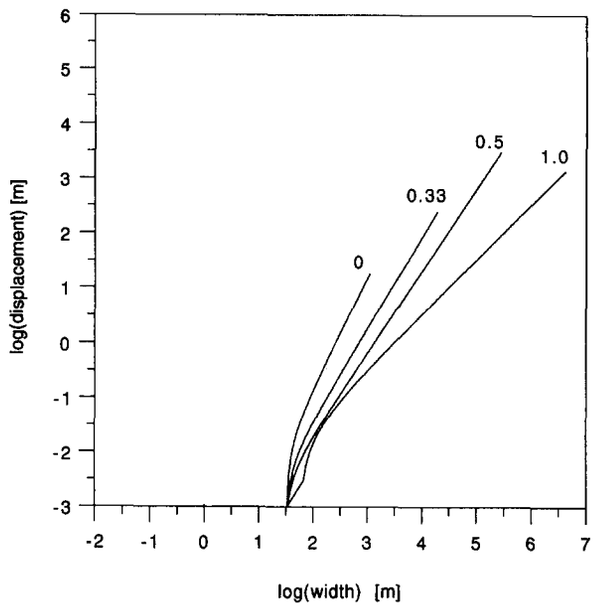

Fig. 12. Growth curves for model in which successive slip increments form a p-series, such that $u_N - u_{N-1} = b(u_{N-1})^i$, for i = 0, 0.33, 0.5 and 1.0. These models provide steady-state growth curves with $n = 2 - i$.

second case (Fig. 12). The second case has a physical basis insofar as the value of the preceding slip event, and hence the slip increment, is linearly related to the fault dimension (W). In this second case, for $i = 0$ slip increments are constant and the successive slip events constitute an arithmetic series and $n = 2.0$. For $i = 1.0$ the slip increment is a linear function of the preceding slip value and successive slip values increase by a constant proportion ($= b$) with each event, i.e. $u_N = (u_{N-1})(1 + b)$, and $n = 1.0$. This model is similar to that of Cowie & Scholz (1992a,b) in which the fault growth increment during a seismic cycle is proportional to the fault dimension, such that $W_N \propto W_{N-1}$. Their model uses a formulation of the Dugdale cohesion zone plate model for inelastic deformation at the tip of a tensile (Mode I) crack, but does not incorporate the relaxation of elastic strains within the entire faulted volume. Application of this model to faults relies largely on qualitative and semi-quantitative observations such as a proposed D vs W relation of $n = 1.0$, which is not borne out by the analysis presented here, and the form of displacement profiles on fault surfaces (see below).

The case of $i = 0.5$, for which $n = 1.5$, is of particular interest as it corresponds to

$$u_N - u_{N-1} = b(u_{N-1})^{0.5} \quad (10)$$

or

$$kW_N - kW_{N-1} = b(kW_{N-1})^{0.5} \quad (11)$$

and

$$W_N - W_{N-1} = (b.k^{-0.5}) \cdot (W_{N-1})^{0.5}, \quad (12)$$

where $b.k^{-0.5}$ is a constant. This model, which we express in terms of fault slip and dimensions, is equivalent to a modification of our previous model suggested by Marrett & Allmendinger (1991), in which the slip increment is linearly related to the number of slip events. Since the stress intensity factor, K_i, is related to the crack dimension (W) by

$$K_i \propto \Delta s.W^{0.5} \text{ (Lawn \& Wilshaw 1975)}, \quad (13)$$

combining these relationships for constant Δs gives

$$W_N - W_{N-1} \propto K_i, \quad (14)$$

i.e. the increase in W for a single event is proportional to the stress intensity factor. Following this model, fracture propagation will occur when the critical stress intensity factor (K_c), or fracture toughness, is exceeded and will continue until the stress intensity factor (K_i) at the tip of the fault reduces to K_c. There is thus a physical basis for $n = 1.5$ which is lacking for other possible growth models based on iterative relaxation of elastic strains.

Preferred value for n

On the basis of data analysis alone the value of n can only be said probably to lie between 1.5 and 2.0; as the angle between lines with these slopes is only 7.1° we think it unlikely that closer resolution can be achieved in the foreseeable future on the basis of data analysis alone. If a preferred value is to be chosen by taking theoretical considerations into account, then $n = 1.5$ seems to us to be the more likely but it is emphasized that significant uncertainty is still attached to this value.

Effects of n *on fault geometries*

The value of n has an effect on some features of the displacement geometry of faults. Using the standard solution for the slip distribution on an elastic dislocation for a single slip event (Eshelby 1957), the effect of fault growth on cumulative displacement profiles can be assessed for different values of n. As the value of n decreases, profiles of cumulative displacement variation on fault surfaces from maximum to zero (Walsh & Watterson 1987) become steeper adjacent to the fault centre, i.e. the displacement decreases more rapidly away from the maximum at the fault centre (Fig. 13a). These cumulative displacement profiles contrast with those predicted by the model of Cowie & Scholz (1992a,b) which show a significant departure from the single slip event profile (Eshelby 1957) only towards the fault tip, where a zone of inelastic deformation is characterized by a reduced displacement gradient. The model of Cowie & Scholz (1992a,b) predicts that a fault maintains a self-similar displacement profile through time,

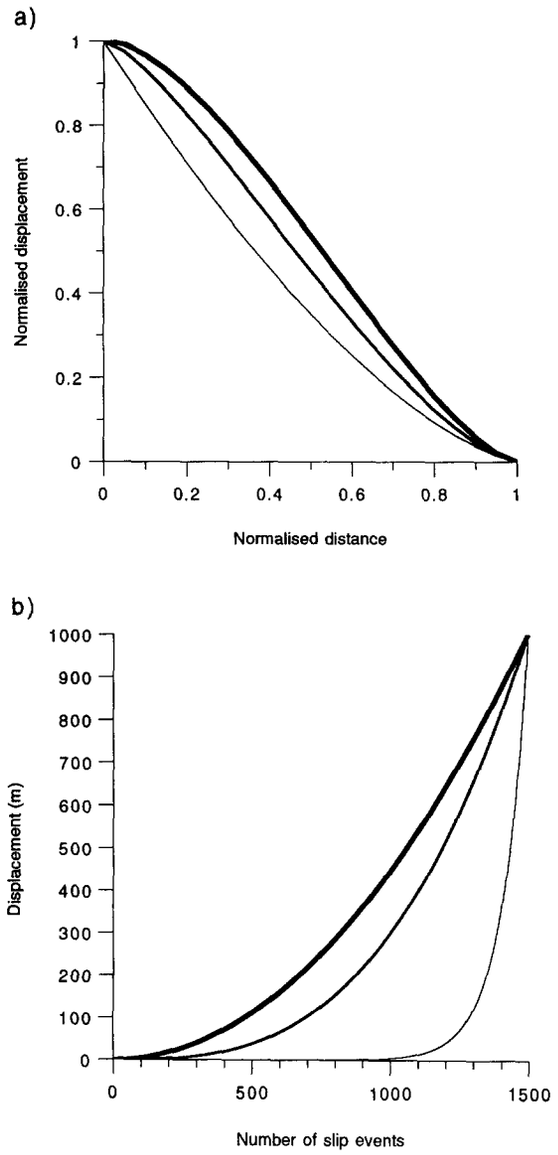

Fig. 13. (a) Normalized displacement profiles from fault centre to fault tip, for growth models with different values of n: 1—fine solid line; 1.5—medium solid line; 2—heavy solid line. Profiles were computed by iteration using the single slip event profile for an elastic dislocation (Eshelby 1957, Walsh & Watterson 1987). (b) Cumulative displacement against number of slip events for growth models with different values of n: 1—fine solid line; 1.5—medium solid line; 2—heavy solid line. In all cases the fault has the same number of slip events (1500) and final displacement (1000 m).

but this result would require a progressive change of the incremental slip profiles during fault growth which is not borne out by observations on neotectonic faults. The form of the displacement profile determines the spacing of depth contours of horizons deformed within the fault volume (Gibson *et al.* 1989) and results in only minor differences in contour patterns between models for $n = 1.5$ and $n = 2.0$.

The partitioning of displacement between successive growth stages of a fault (Gibson *et al.* 1989) is also determined by the value of n. Figure 13(b) shows the relative rates of displacement at different stages of fault growth for different values of n and assuming that each seismic cycle occupies the same amount of time. The exponential increase in relative growth rate for the case

of $n = 1.0$ is unrealistic (Fig. 13b), whereas the differences between the relative growth rates for $n = 1.5$ and $n = 2.0$ are relatively insignificant. The assumption that each seismic cycle occupies the same time (Gibson *et al.* 1989) is probably incorrect because it is based on the assumption of constant earthquake recurrence intervals throughout the life of a fault. Recurrence intervals may increase with fault size (Walsh & Watterson 1992) but this is unlikely to affect the relative differences in growth rate patterns described above. Reference to earthquake recurrence intervals should not be taken as implying that the conclusions apply only to seismic faults as the earthquake recurrence intervals are simply an expression of the time-averaged rates of release of strain energy. The displacement population (Childs *et al.* 1990) of a single fault surface will also vary with the value of n (Walsh *et al.* 1991) but there is no significant difference when the populations are plotted on the conventional log–log plot of cumulative number vs displacement.

CONCLUSIONS

(1) Displacement-dimension data for *ca* 1350 individual faults are available with maximum displacements ranging over 8 orders of magnitude.

(2) Maximum displacements and dimensions of faults are related by a power law with exponent n.

(3) Because variables other than D and W are significant, departures from a straight line relationship are to be expected and the data cannot be analysed satisfactorily by standard statistical methods.

(4) Data spanning several orders of magnitude of fault dimension must be examined in order to overcome the effects of the noise resulting from additional variables.

(5) Log–log plots of the data are necessary but much of the plots represent values which in practice are unobtainable and concentrations of data points must be interpreted with this restriction in mind.

(6) Suggestions that the value of the power-law exponent is 1.0 are not consistent with the data, but the data are not sufficiently precise to distinguish, on the basis of data analysis alone, between values of 1.5 and 2.0 for the exponent.

(7) An exponent of 1.5 is consistent with a growth model which has a reasonable mechanical basis in that the growth of the linear dimension of a fault in each growth event is proportional to the square root of the dimension; 1.5 is therefore the preferred value for the exponent.

(8) Geometrical characteristics of faults which are influenced by the value of the exponent are displacement profiles on fault surfaces, depth contour patterns and spacings for faulted horizons, and displacement populations on surfaces of single faults. The differences in these geometrical characteristics between $n = 1.5$ and $n = 2.0$ are relatively minor.

Acknowledgements—Members of the Liverpool Fault Analysis Group are thanked for their assistance with collation and analysis of the data. We thank Henning Omre for discussions on the statistical analysis of the data. The work was carried out as a part of projects funded by the E.C. JOULE Programme (contract JOUF-0036-C) and the N.E.R.C. Petroleum Earth Sciences Programme (grant D1/G1/189/03).

REFERENCES

Babenroth, D. L. & Strahler, A. N. 1945. Geomorphology and structure of the East Kaibab Monocline, Arizona and Utah. *Bull. geol. Soc. Am.* **56**, 107–150.

Barnett, J. A. M., Mortimer, J., Rippon, J. H., Walsh, J. J. & Watterson, J. 1987. Displacement geometry in the volume containing a single normal fault. *Bull. Am. Ass. Petrol. Geol.* **71**, 925–937.

Childs, C., Walsh, J. J. & Watterson, J. 1990. A method for estimating the density of fault displacements below the limit of seismic resolution in reservoir formations. In: *North Sea Oil and Gas Reservoirs II* (edited by The Norwegian Institute of Technology). Graham & Trotman, London, 309–318.

Cowie, P. A. & Scholz, C. H. 1992a. Physical explanation for the displacement-length relationship of faults using a post-yield fracture mechanics model. *J. Struct. Geol.* **14**, 1133–1148.

Cowie, P. A. & Scholz, C. H. 1992b. Growth of faults by accumulation of seismic slip. *J. geophys. Res.* **97**, 11,085–11,096.

Davis, J. C. 1986. *Statistics and Data Analysis in Geology* (2nd edn). Wiley & Sons, New York.

Elliott, D. 1976. Energy balance and deformation mechanisms of thrust sheets. *Phil. Trans. R. Soc. Lond.* **A283**, 289–312.

Eshelby, J. D. 1957. The determination of the elastic field of an ellipsoidal inclusion and related problems. *Phil. Trans. R. Soc. Lond.* **A241**, 376–396.

Gibson, J. R., Walsh, J. J. & Watterson, J. 1989. Modelling of bed contours and cross-sections adjacent to planar normal faults. *J. Struct. Geol.* **11**, 317–328.

Gillespie, P. A. In press. Displacement variations of thrusts, normal faults and folds from the Ruhr and the South Wales Coalfields. In: *Rhenohercynian and Subvariscan Fold Belts* (edited by Gayer, R. A. & Greiling, R.).

Kanamori, H. & Anderson, D. L. 1975. Theoretical basis of some empirical relations in seismology. *Bull. seism. Soc. Am.* **65**, 1073–1095.

Krantz, R. W. 1988. Multiple fault sets and three-dimensional strain: Theory and application. *J. Struct. Geol.* **10**, 225–237.

Larsen, P. -H. 1988. Relay structures in a Lower Permian basement-involved extension system, East Greenland. *J. Struct. Geol.* **10**, 3–8.

Lawn, B. R. & Wilshaw, T. R. 1975. *Fracture of Brittle Solids*. Cambridge University Press, Cambridge.

MacMillan, R. A. 1975. The orientation and sense of displacement of strike-slip faults in continental crust. Unpublished B.S. thesis, Carleton University, Ottawa, Ontario.

Marrett, R. & Allmendinger, R. W. 1991. Estimates of strain due to brittle faulting: sampling of fault populations. *J. Struct. Geol.* **13**, 735–738.

Menard, H. W. 1962. Correlation between length and offset on very large wrench faults. *J. geophys. Res.* **67**, 4096–4098.

Minor Faults Research Group (MFRG). 1973. A minor fault system around the Otaki area, Boso Peninsula, Japan. *Earth Sci. (Chikyu Kagaku)* **27**, 180–187.

Muraoka, H. & Kamata, H. 1983. Displacement distribution along minor fault traces. *J. Struct. Geol.* **5**, 483–495.

Opheim, J. A. & Gudmundsson, A. 1989. Formation and geometry of fractures, and related volcanism, of the Krafla fissure swarm, northeast Iceland. *Bull. geol. Soc. Am.* **101**, 1608–1622.

Peacock, D. C. P. 1991. Displacements and segment linkage in strike-slip fault zones. *J. Struct. Geol.* **13**, 1025–1035.

Peacock, D. C. P. & Sanderson, D. J. 1991. Displacements, segment linkage and relay ramps in normal fault zones. *J. Struct. Geol.* **13**, 721–733.

Ranalli, G. 1977. Correlation between length and offset in strike-slip faults. *Tectonophysics* **37**, T1–T7.

Ranalli, G. 1980. A stochastic model for strike-slip faulting. *Math. Geol.* **12**, 399–412.

Ruzhich, V. V. 1977. Relations between fault parameters and practical application of them. In: *Mekhanizmy Structur Vostochnochnoisibiri Novisbirsk Nanka* (in Russian).

Schwartz, D. P. & Coppersmith, K. J. 1984. Fault behaviour and characteristic earthquakes: Examples from the Wasatch and San Andreas fault zones. *J. geophys. Res.* **89**, 5681–5698.

Scholz, C. H. 1982. Scaling laws for large earthquakes; consequences for physical models. *Bull. seism. Soc. Am.* **72**, 1–14.

Scholz, C. H., Aviles, C. A. & Wesnousky, S. G. 1986. Scaling differences between large interplate and intraplate earthquakes. *Bull. seism. Soc. Am.* **76**, 65–70.

Scholz, C. H. 1990. *The Mechanics of Earthquakes and Faulting*. Cambridge University Press, Cambridge.

Scholz, C. H. & Cowie, P. A. 1990. Determination of total strain from faulting using slip measurements. *Nature* **346**, 837–839.

Strelau, J. 1986. A discussion of the depth extent of rupture in large continental earthquakes. In: *Earthquake Source Mechanics* (edited by Das, S., Boatwright, J. & Scholz, C. H.). *Am. Geophys. Monogr.* **37**, *Maurice Ewing Volume* **6**, 131–146.

Thompson, D. W. 1917. *On Growth and Form*. Cambridge University Press, Cambridge.

Villemin, T. & Sunwoo, C. 1987. Distribution logarithmique self-similaire des rejets et longueurs de failles: exemple du Bassin Houiller Lorrain. *C. r. Acad. Sci., Paris* **305**, 1309–1312.

Walsh, J. J. & Watterson, J. 1987. Distributions of cumulative displacement and seismic slip on a single normal fault surface. *J. Struct. Geol.* **9**, 1039–1046.

Walsh, J. J. & Watterson, J. 1988. Analysis of the relationship between displacements and dimensions of faults. *J. Struct. Geol.* **10**, 239–247.

Walsh, J. J. & Watterson, J. 1989. Displacement gradients on fault surfaces. *J. Struct. Geol.* **11**, 307–316.

Walsh, J. J. & Watterson, J. 1990. New methods of fault projection for coalmine planning. *Proc. Yorks. geol. Soc.* **48**, 209–219.

Walsh, J. J. & Watterson, J. 1991. Geometric and kinematic coherence and scale effects in normal fault systems. In: *Geometry of Normal Faults* (edited by Roberts, A. M., Yielding, G. & Freeman, B.). *Spec. Publs geol. Soc. Lond.* **56**, 193–203.

Walsh, J. J., Watterson, J. & Yielding, G. 1991. The importance of small-scale faulting in regional extension. *Nature* **351**, 391–393.

Walsh, J. J. & Watterson, J. 1992. Populations of faults and fault displacements and their effects on estimates of fault-related regional extension. *J. Struct. Geol.* **14**, 701–712.

Watterson, J. 1986. Fault dimensions, displacements and growth. *Pure & Appl. Geophys.* **124**, 365–373.

Wesnousky, S. G., Scholz, C. H., Shimazaki, K. & Matsuda, T. 1983. Earthquake frequency distribution and mechanics of faulting. *J. geophys. Res.* **88**, 9331–9340.